Capillarity

Vol. 4, No. 1, p. 13-22, 2021

Original article

Prediction of spontaneous imbibition in fractal porous media based on modified porosity correlation

Yinglin Li*, Di Yu, Baolian Niu

School of Energy and Mechanical Engineering, Nanjing Normal University, Nanjing 210000, P. R. China

Keywords:
Spontaneous imbibition
capillary pressure
fractal theory
porous media

Cited as:
Li, Y., Yu, D., Niu, B. Prediction of spontaneous imbibition in fractal porous media based on modified porosity correlation. Capillarity, 2021, 4(1): 13-22, doi: 10.46690/capi.2021.01.02

Abstract:
Spontaneous imbibition plays a significant role in different technical applications, and several analytical models have been proposed for predicting the fluid imbibition mass into porous media based on the fractal theory. Herein, these previous models are reconsidered in view of the obvious difference between the effective porosity and the areal porosity of porous media. Firstly, an implicit equation for fractal tortuosity is proposed and a modified correlation for the areal porosity is presented; then, a semi-analytical prediction model for fluid imbibition mass with gravity pressure is derived; finally, comparisons of predictions among several previous models with the present model are carried out. The modeling results show consistency with the experimental data published in the literature.

1. Introduction

The phenomenon of spontaneous imbibition, which is driven by capillary pressure, has an important function in different technical applications, such as oil recovery (Gao et al., 2018), carbon dioxide storage by capillary trapping (Arshad et al., 2016), paper sensors (Elizalde et al., 2015), inkjet printing (Wijshoff, 2017), heat pipe wicks (Nishikawara et al., 2018), or microfluidic devices (Dudek et al., 2018). There is great research interest in spontaneous imbibition in porous media (Ashraf et al., 2019). One of the 'hot topics' is to predict the fluid imbibition mass (Liu et al., 2020; Orlando et al., 2020).

The widely known Lucas-Washburn (LW) equation (Lucas, 1918; Washburn, 1921) indicated that the imbibition distance and mass versus the time followed the correlation of $t^{0.5}$ in a circular capillary. However, there existed much controversy over the availability of LW equation, and some studies argued that the imbibed mass could not hold the correlation of $t^{0.5}$; therefore, many studies derived new versions of this equation to cohere with testing results, as discussed in a comprehensive review in the literature (Cai and Yu, 2011).

The fractal theory is of great interest when studying fluid flow in porous media, as well as for the analysis of rock properties, such as the roughness of rock surface (Xie et al., 2020), porosity (Pia et al., 2013), permeability (Mahabadi et al., 2019), tortuosity (Comiti and Renaud, 1989) and capillary pressure (Li, 2010).

Regarding the spontaneous imbibition in fractal porous media, Li and Zhao (2012) early proposed a mathematical model to predict the fluid imbibition mass, and presented the power law relationship between imbibition mass and time. They argued that the time exponent lied in the range of 0 to 1. Balankin et al. (2012) carried out experiments and a theoretical analysis on fluid impregnation in porous media, and considered the time exponents as usually less than 0.5. Cai et al. (2010a) analyzed capillary imbibition in a single curving capillary based on the fractal theory and presented an analytical solution for the height of fluid imbibition. Subsequently, an analytical solution for spontaneous imbibition mass in porous media was proposed (Cai et al., 2010b), it indicated that the fractal character had an obvious effect on fluid imbibition height. Cai et al. (2010c) then derived the correlations of the depth of fluid invasion based on fractals, and proposed that capillary

*Corresponding author.
E-mail address: ylli@njnu.edu.cn (Y. Li); yudi1310@163.com (D. Yu); niubaolian@163.com (B. Niu).

Yandy Scientific Press

2709-2119
Received February 18, 2021; revised March 9, 2021; accepted March 9, 2021; available online March 12, 2021.

tortuosity and pressure effect were the two key factors for analyzing the extraneous invasion in porous media with lower porosity. Cai and Yu (2011) studied the influence of fractal tortuosity on spontaneous imbibition mass in porous media and suggested that the time exponent was within 0.167 to 0.5. Cai et al. (2012) treated the porous media as a bundle of tortuous capillaries, and constructed a mathematical model of spontaneous imbibition on the condition of gravitational pressure. Based on the previous studies above, Shi et al. (2018) assumed that the front of the fluid imbibition process was not uniform, and that the fluid inside capillaries with different diameters spent different time periods before arriving at the top of the rock sample. Therefore, they derived a new semi-analytical model for spontaneous imbibition in porous media on the condition of gravity pressure.

However, in attempts to explain spontaneous imbibition based on the fractal theory, the difference between the areal porosity ϕ_a and the effective porosity ϕ_c had been studied with much less intensity, and only a few researches had focused on this issue. Yu et al. (2009) clearly suggested that the areal porosity ϕ_a of porous media was a two-dimensional parameter, whereas the effective porosity ϕ_c of porous media was a three-dimensional parameter, and the correlations for the corresponding two kinds of porosity were entirely different. Other studies either simply considered ϕ_a as ϕ_c (Cai et al., 2014), or merely regarded ϕ_c as the product of areal porosity ϕ_a and average capillary tortuosity τ_{av} (Shi et al., 2018). In this work, according to the definition of porosity (Yu et al., 2009), a modified correlation for ϕ_a is derived, the important distinction between ϕ_c and ϕ_a is further discussed, and a new semi-analytical model of spontaneous imbibition with gravity is proposed.

This paper is organized as follows: a mathematical model of the co-current spontaneous imbibition process is derived in Section 2. The unknown parameter derivation and logic computational procedure are discussed in Section 3. Predictions of the present model and previous models are compared with the testing data of previous studies in Section 4. Finally, Section 5 concludes the paper with a summary of the main results.

2. Model of spontaneous imbibition in fractal porous media

In this section, firstly, the fractal characteristics of porous media are introduced; then, a mathematical model of the spontaneous imbibing process in a single tortuous capillary is derived; finally, a semi-analytical prediction model of the spontaneous imbibing process in a bundle of tortuous capillaries is proposed.

2.1 Fractal characteristics of porous media

Since precise self-similar fractals are relatively rare in nature, the porous media are characterized by statistical self-similar fractals. Thus, the total number N of pores with diameter not less than the size λ in the cross section area A_u follows the fractal power law (Yu and Cheng, 2002). The total cross section area A_u of the cubic unit cell, as shown in Fig. 1, can be formulated as follows (Wu and Yu, 2007):

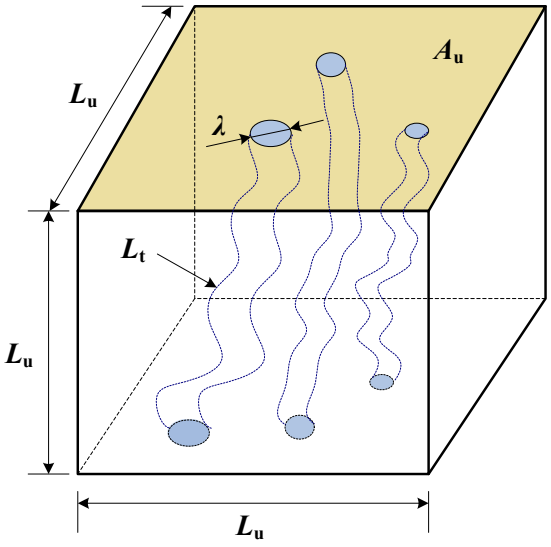

Fig. 1. Structure of cubic unit cell with side length L_u.

$$A_u = \frac{-\int_{\lambda_{min}}^{\lambda_{max}} \frac{\pi\lambda^2}{4} dN}{\phi_a} = \frac{\pi\lambda_{max}^2 D_f}{4(2-D_f)} \frac{1-\xi^{2-D_f}}{\phi_a} \tag{1}$$

where λ represents the pore diameter of capillary, λ_{max} is the maximum pore diameter, D_f represents the pore fractal dimension of this unit cell, ξ denotes the ratio of λ_{min} to λ_{max}, and ϕ_a is the areal porosity (in two dimensions) of the cross section of the cubic unit cell.

The total number of capillaries with diameter not less than λ in a rock sample (N_t) can be calculated as follows (Cai et al., 2012):

$$N_t(\geq \lambda) = \frac{4(2-D_f)}{\pi D_f \lambda_{max}^{2-D_f}} \frac{A_s \phi_a}{1-\xi^{2-D_f}} \lambda^{-D_f} \tag{2}$$

where A_s is the total cross section area of the rock sample, and the value of A_s is commonly far greater than the value of A_u.

2.2 Spontaneous imbibition in a single tortuous capillary

As shown in Fig. 2, assuming that the incompressible Newtonian fluid flows up along a tortuous capillary (Liu et al., 2014), the fluid can successfully extend from the bottom surface to the top surface of the rock sample for a typical capillary (such as C1 or C2), while the fluid fails to reach the top surface and its outlet connects with the side surface of rock sample for an atypical capillary (such as C3).

In the following analysis, we ignore the atypical capillaries (such as C3 in Fig. 2), and assume that all capillaries can successfully extend from the bottom to the top surface of the rock sample. The imbibition process follows the Hagen-Poiseuille law (Cai and Yu, 2011):

$$\frac{dL_t}{dt} = \frac{Q_s}{\pi\lambda^2/4} = \frac{\lambda^2}{32\mu L_t}\left(\frac{4\sigma\cos\theta}{\lambda} - \rho g L_s\right) \tag{3}$$

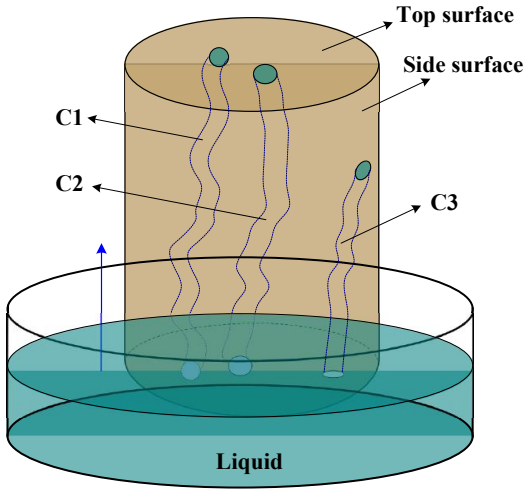

Fig. 2. View of co-current spontaneous imbibing process in rock sample.

where Q_s represents the fluid volumetric flow rate in a single capillary with diameter λ; L_t and L_s represent actual tortuous distance and straight distance of the fluid column inside the capillary, respectively; t denotes the fluid imbibing time, σ represents surface tension, θ is the contact angle, μ indicates fluid viscosity, ρ is fluid density, g represents gravitational acceleration, and $\rho g L_s$ is the gravitational pressure of liquid column in the capillary.

1) When the gravitational pressure can be ignored compared to the capillary pressure, inserting the correlation of $L_t = \lambda^{1-D_t} L_s^{D_t}$ into Eq. (3) yields the formula (Cai et al., 2010a; Cai and Yu, 2011):

$$L_s = \left(\frac{\lambda^{2D_t-1}\sigma\cos\theta}{4\mu}\right)^{\frac{1}{2D_t}} t^{\frac{1}{2D_t}} \tag{4}$$

2) When the gravitational pressure cannot be neglected compared to the capillary pressure, obtaining the exact analytical solution of L_s against time according to Eq. (3) is very difficult. Here, a numerical calculating method is adopted for solving Eq. (3). As the imbibing process proceeds from the time interval t_{i-1} to t_i, the straight distance of fluid column correspondingly increases from $L_{s,i-1}$ to $L_{s,i}$, where t_{i-1} and t_i represent the previous time and the current time, respectively. Integrating Eq. (3) from the $(i-1)^{\text{th}}$ time step to the i^{th} one (Shi et al., 2018) yields:

$$\int_{L_{s,i-1}}^{L_{s,i}} L_s^{D_t} dL_s^{D_t} = \int_{t_{t-1}}^{t_i} \left(\frac{\lambda^{2D_t-1}\sigma\cos\theta}{8\mu} - \frac{\rho g\lambda^{2D_t}L_s}{32\mu}\right) dt \tag{5}$$

The second item 'L_s' on the right side of Eq. (5) is assumed to be equal to $L_{s,i-1}$ for a time interval (dt) that is small enough. Based on Eq. (5), one can obtain the formula (Shi et al., 2018):

$$L_{s,i} = \left[L_{s,i-1}^{2D_t} + \left(\frac{\lambda^{2D_t-1}\sigma\cos\theta}{4\mu} - \frac{\rho g\lambda^{2D_t}L_{s,i-1}}{16\mu}\right)\Delta t\right]^{\frac{1}{2D_t}} \tag{6}$$

where $i = 1, 2, \ldots, nt$; the parameter nt is the total interval number, and $L_{s,0} = 0$. The value of time interval is $\Delta t = t/nt$. The first time step ($i = 1$) corresponds to the initial imbibition process when the bottom surface of the capillary has just been moistened by the fluid; the last time step ($i = nt$) represents that the imbibition process is about to terminate, and at this time, the corresponding distance of the fluid column ($L_{s,nt}$) represents the final fluid height associated with the given imbibition time t.

The value of $L_{s,nt}$ can be obtained by using the method of iterative calculations, and the total imbibed mass of fluid in the single capillary, $m(\lambda)$, is calculated as:

$$m(\lambda) = \frac{\rho\pi\lambda^{3-D_t}}{4}\left[L_{s,nt-1}^{2D_t} + \left(\frac{\lambda^{2D_t-1}\sigma\cos\theta}{4\mu} - \frac{\rho g\lambda^{2D_t}L_{s,nt-1}}{16\mu}\right)\Delta t\right]^{\frac{1}{2}} \tag{7}$$

2.3 Spontaneous imbibition in a bundle of tortuous capillaries

In this part, a co-current spontaneous imbibing model of fluid in the capillary bundle is proposed by viewing the porous media as an ideal bundle of capillaries with different diameters.

2.3.1 Spontaneous imbibition without considering gravity

The spontaneous imbibing process of fluid in the capillary bundle is analyzed here while ignoring gravitational pressure.

In the section, we analyze the spontaneous imbibing process of fluid in the capillary bundle with ignoring gravitational pressure. By differentiating Eq. (2) with respect to λ, we can get the capillary number with diameter value in the scope of λ to $\lambda + d\lambda$.

$$-dN_t(\geq\lambda) = \frac{4A_s}{\pi\lambda_{\max}^{2-D_f}}\frac{(2-D_f)\phi_a}{1-\xi^{2-D_f}}\lambda^{-D_f-1}d\lambda \tag{8}$$

Through combining Eq. (4) and Eq. (8), the total imbibed mass of fluid in the capillaries within the scope of λ to $\lambda + d\lambda$ can be given as:

$$M(\lambda) = \frac{\rho A_s}{2\lambda_{\max}^{2-D_f}}\frac{(2-D_f)\phi_a}{1-\xi^{2-D_f}}\sqrt{\frac{\sigma t\cos\theta}{\mu}}\lambda^{1.5-D_f}d\lambda \tag{9}$$

Eq. (9) is valid only when the imbibed fluid in the capillary has not reached the top surface of the rock sample. Once the fluid has reached the top surface, the fluid imbibition process terminates, and the total imbibed fluid mass should be revised as equilibrated mass at this time:

$$\begin{aligned} M_e(\lambda) &= \rho\frac{\pi}{4}\lambda^2\lambda^{1-D_t}H^{D_t}(-dN_t) \\ &= \frac{\rho H^{D_t}A_s}{\lambda_{\max}^{2-D_f}}\frac{(2-D_f)\phi_a}{1-\xi^{2-D_f}}\lambda^{2-D_t-D_f}d\lambda \end{aligned} \tag{10}$$

where M_e represents the total equilibrated fluid mass in the capillaries within the scope of λ to $\lambda + d\lambda$, and H represents the vertical height of the rock sample.

The total imbibed fluid mass inside all of the capillaries (M_t) within the given imbibing time can be formulated by combining Eq. (9) and Eq. (10) (Shi et al., 2018):

$$M_t = \int_{\lambda_{\min}}^{\lambda_c} M(\lambda) + \int_{\lambda_c}^{\lambda_{\max}} M_e(\lambda) \tag{11}$$

where the critical diameter λ_c is the diameter of capillaries that have just been fully fed with fluid at the given imbibing time t. Based on Eq. (4), the fluid in larger capillaries fills them faster than smaller capillaries for the same imbibing time. Therefore, the imbibition process in any capillary with diameter larger than the value of λ_c ceases at this moment. The parameter λ_c can be solved by substituting L_s with H in Eq. (4) as follows:

$$\lambda_c = \left(\frac{4\mu H^{2D_t}}{t\sigma\cos\theta}\right)^{\frac{1}{2D_t-1}} \tag{12}$$

Eq. (12) indicates that λ_c is a time-dependent parameter that decreases with time t. At the initial spontaneous imbibition process, λ_c may be far greater than $\lambda_{\max}$, whereas at the final spontaneous imbibition process, λ_c may be smaller than $\lambda_{\min}$.

For the case of $\lambda_c > \lambda_{\max}$, namely, when the fluid imbibing process is at the initial stage, $\lambda_c = \lambda_{\max}$ should be set in Eq. (11), and then Eq. (11) can be modified as:

$$\begin{aligned} M_t &= \int_{\lambda_{\min}}^{\lambda_{\max}} M(\lambda) \\ &= \frac{\rho A_s\left(2-D_f\right)}{5-2D_f}\frac{\phi_a\lambda_{\max}^{1/2}}{1-\xi^{2-D_f}}\sqrt{\frac{\sigma t\cos\theta}{\mu}}\left(1-\xi^{2.5-D_f}\right) \end{aligned} \tag{13}$$

For the case of $\lambda_c < \lambda_{\min}$, namely, when the fluid front reaches the top of all capillaries and the fluid imbibition process has already stopped, $\lambda_c = \lambda_{\min}$ should be set in Eq. (11), and then Eq. (11) is changed as follows:

$$\begin{aligned} M_t &= \int_{\lambda_{\min}}^{\lambda_{\max}} M_e(\lambda) \\ &= \frac{\rho H^{D_t} A_s}{1-\xi^{2-D_f}}\frac{\left(2-D_f\right)\phi_a\lambda_{\max}^{1-D_t}}{3-D_t-D_f}\left(1-\xi^{3-D_t-D_f}\right) \end{aligned} \tag{14}$$

From Eq. (12), it can be seen that the condition of $\lambda_c < \lambda_{\min}$ will certainly occur when the given imbibition time t is long enough. This means that, without considering gravity, the fluid imbibed in any capillary can finally reach the top of the rock sample as long as the imbibition time is sufficient.

2.3.2 Spontaneous imbibition while considering gravity

In this part we analyze the spontaneous imbibing process of fluid in a capillary bundle on the condition of gravitational pressure. Eq. (8) can be transformed into:

$$\Delta N_t(\geq\lambda) = \frac{4A_s}{\pi\lambda_{\max}^{2-D_f}}\frac{\left(2-D_f\right)\phi_a}{1-\xi^{2-D_f}}\lambda^{-D_f-1}\Delta\lambda \tag{15}$$

where $\Delta\lambda$ represents the diameter interval, and ΔN_t denotes the number of capillaries with diameter value in the range of λ to $\lambda+\Delta\lambda$.

Based on Eq (15), we can obtain:

$$\begin{aligned} M(\lambda) =& \rho\frac{\pi}{4}\lambda^2\lambda^{1-D_t}L_{s,nt}^{D_t}\Delta N_t \\ =& \left[L_{s,nt-1}^{2D_t}+\left(\frac{\lambda^{2D_t-1}\sigma\cos\theta}{4\mu}-\frac{\rho g\lambda^{2D_t}L_{s,nt-1}}{16\mu}\right)\Delta t\right]^{\frac{1}{2}} \\ &\times\frac{2-D_f}{\lambda_{\max}^{2-D_f}}\frac{\rho A_s\phi_a\lambda^{2-D_t-D_f}}{1-\xi^{2-D_f}}\Delta\lambda \end{aligned} \tag{16}$$

It should be noted that the value of nt in Eq. (16) is a self-defined variable constant for different imbibition times; while the given time t increases, the value of nt rises to a larger constant. This can prove that the time interval ($\Delta t = t/nt$) can be small enough while the given time t varies. For example, when the imbibition time t is limited to 50 s, $nt = 500$, $\Delta t = 0.1$ s, while time t is defined as 1000 s, $nt = 10000$, and Δt can still be equal to 0.1 s.

Eq. (16) is valid only if the imbibing fluid column in the capillary has not reached the top surface of the rock sample. When combining with Eq. (15), the equilibrated imbibed mass (M_e) in the bundle with diameter in the range of λ to $\lambda+\Delta\lambda$. is calculated by the formula:

$$\begin{aligned} M_e(\lambda) &= \rho\frac{\pi}{4}\lambda^2\lambda^{1-D_t}H^{D_t}\Delta N_t \\ &= \frac{2-D_f}{\lambda_{\max}^{2-D_f}}\frac{\rho A_s H^{D_t}\phi_a\lambda^{2-D_t-D_f}}{1-\xi^{2-D_f}}\Delta\lambda \end{aligned} \tag{17}$$

Combining Eq. (16) and Eq. (17) yields the total imbibed fluid mass inside all capillaries within the given imbibition time, as follows:

$$\begin{aligned} M_t =& \sum_{j=\lambda_{\min}}^{\lambda_c}\left[L_{s,nt-1}^{2D_t}+\left(\frac{j^{2D_t-1}\sigma\cos\theta}{4\mu}-\frac{\rho g j^{2D_t}L_{s,nt-1}}{16\mu}\right)\Delta t\right]^{\frac{1}{2}} \\ &\times\frac{2-D_f}{\lambda_{\max}^{2-D_f}}\frac{\rho A_s\phi_a j^{2-D_t-D_f}}{1-\xi^{2-D_f}}\Delta j \\ &+\sum_{j=\lambda_c+\Delta\lambda}^{\lambda_{\max}}\frac{2-D_f}{\lambda_{\max}^{2-D_f}}\frac{\rho A_s H^{D_t}\phi_a j^{2-D_t-D_f}}{1-\xi^{2-D_f}}\Delta j \end{aligned} \tag{18}$$

It should be noted that the critical diameter λ_c in Eq. (12) is not suitable for Eq. (18). And the new value of λ_c in Eq. (18) can be obtained by substituting $L_{s,nt}$ with H in the left side of Eq. (6) while $i = nt$.

From Eq. (3), we can derive that the spontaneous imbibition process ceases when the gravitational pressure equals to the capillary pressure, and there exists an exact threshold diameter λ_t (Shi et al., 2018). By defining $dL_t/dt = 0$ in Eq. (3), we can obtain:

$$\lambda_t = \frac{4\sigma\cos\theta}{\rho g H} \tag{19}$$

When $\lambda < \lambda_t$, the spontaneous imbibition process continues, and the fluid front of the capillary with diameter λ finally reaches the top surface of the rock sample, as long as the imbibition time is long enough. On the contrary, when $\lambda > \lambda_t$, the spontaneous imbibition process stops at a certain height,

because the fluid front cannot reach the top surface of the rock sample.

3. Parameter derivation and computational procedure

Eqs. (11) and (18) are the final solutions for describing the spontaneous imbibition of fluid into a capillary bundle with and without gravitational pressure, respectively. In Eqs. (11) and (18), ρ, σ, θ, μ, A_s, H and ϕ_c are known parameters; and $\lambda_{\max}$, $\lambda_{\min}$, D_f, D_t and ϕ_a are unknown parameters. This section will determine the five unknown parameters.

Firstly, the value of $\lambda_{\max}$ can be obtained by the mathematical correlation for maximum pore diameter (Cai et al., 2010b), and $\lambda_{\min}$ can be acquired based on the correlation of $\lambda_{\max}/\lambda_{\min}=0.01$ (Yu et al., 2009; Cai et al., 2010c). The value of fractal tortuosity dimension D_t can be calculated by the formula:

$$D_t = 1 + \frac{\ln\left(1-a\ln\phi_c\right)}{\ln\left\{\left[\frac{\pi D_f}{4\left(3-D_t-D_f\right)\phi_c}\left(1-\xi^{3-D_t-D_f}\right)\right]^{\frac{1}{3-D_t}}\frac{D_f-1}{\xi D_f}\right\}} \tag{20}$$

where the parameter a is a fitting constant, $a=0.41$ for the spherical particles, and $a=0.63$ for the cubic particles (Comiti and Renaud, 1989).

Eq. (20) is clearly an implicit equation that cannot be solved directly. Once the parameters $\lambda_{\max}$, $\lambda_{\min}$, D_f and ϕ_c have been obtained, the value of D_t can be calculated based on the implicit Eq. (20) by using the iteration method. The calculated results will be analyzed in Section 4.

It is worth mentioning that previous studies (Yu and Cheng, 2002; Cai et al., 2012) considered that the effective porosity ϕ_c (in three dimensions) was equal to the areal porosity ϕ_a (in two dimensions). However, Shi et al. (2018) argued that ϕ_c was equal to the product of τ_{av} and ϕ_a, while Cai and Yu (2011) found that the value of ϕ_c was equal to the value of ϕ_a only on the condition that the capillaries were straight ($\tau_{av}=1$).

For a cubic unit cell, the areal porosity ϕ_a in two dimensions can be expressed as follows (Yu et al., 2009):

$$\phi_a = \frac{\pi D_f}{4\left(2-D_f\right)}\left(\frac{\lambda_{\max}}{L_u}\right)^2\left(1-\xi^{2-D_f}\right) \tag{21}$$

where L_u represents the side length of the cubic unit cell (as shown in Fig. 1). The effective porosity ϕ_c can defined as the ratio of the pore volume of cubic unit cell to the whole volume of cubic unit cell, and is given as follows (Yu et al., 2009):

$$\phi_c = \frac{\pi D_f}{4\left(3-D_t-D_f\right)}\left(\frac{\lambda_{\max}}{L_u}\right)^{3-D_t}\left(1-\xi^{3-D_t-D_f}\right) \tag{22}$$

When comparing Eq. (21) with Eq. (22), we find that the value of ϕ_a is different from the value of ϕ_c while considering the tortuosity dimension D_t. Furthermore, we can observe that the ratio of ϕ_c to ϕ_a is not equal to the value of tortuosity τ_{av}. This is a deviation from the correlation developed by Shi et al. (2018), and $\phi_c=\phi_a$ is only true on the condition of $D_t=1$.

Based on Eq. (22), the ratio of $\lambda_{\max}/L_u$ in three dimensions can be obtained as:

$$\frac{\lambda_{\max}}{L_u} = \left[\frac{4\left(3-D_t-D_f\right)\phi_c}{\pi D_f\left(1-\xi^{3-D_t-D_f}\right)}\right]^{\frac{1}{3-D_t}} \tag{23}$$

Inserting Eq. (23) into Eq. (21) yields a modified correlation for effective porosity:

$$\phi_a = \left[\frac{4\left(3-D_t-D_f\right)\phi_c}{\pi D_f\left(1-\xi^{3-D_t-D_f}\right)}\right]^{\frac{2}{3-D_t}}\frac{\pi D_f\left(1-\xi^{2-D_f}\right)}{4\left(2-D_f\right)} \tag{24}$$

In this paper, the value of effective porosity ϕ_a is calculated according to Eq. (24).

In summary, in order to calculate the total imbibed fluid mass while considering gravity, we firstly insert the known parameters ρ, σ, θ, μ, A_s, H and ϕ_c into the equations above, the unknown parameters, such as $\lambda_{\max}$, $\lambda_{\min}$, D_f, D_t and ϕ_a, can be calculated; then, we can calculate $-\Delta N_t$ by Eq. (15), $L_{s,i}$ by Eq. (6), $M(\lambda)$ by Eq. (16) or $M_e(\lambda)$ by Eq. (17); finally, we can obtain the value of M_t by using Eq. (18). The detailed calculation procedure for obtaining the total imbibed fluid mass while considering gravity is proposed in Fig. 3. It is should be noted that, in Fig. 3, $nt=t/\Delta t$, $\Delta\lambda=\lambda_{\min}/10$, and $\lambda_{\min}\le j\le\lambda_{\max}$.

In order to further analyze the prediction of imbibition mass by Eq. (18), two typical prediction models of spontaneous imbibition while considering gravity will be further analyzed in Section 4. The first one (Shi et al., 2018) is the following:

$$\begin{aligned} M_t = &\sum_{j=\lambda_{\min}}^{\lambda_c}\left[\left(\tau_{av}L_{s,nt-1}\right)^2+\left(\frac{j\sigma\cos\theta}{4\mu}-\frac{\rho g j^2 L_{s,nt-1}}{16\mu}\right)\Delta t\right]^{1/2} \\ &\times\frac{2-D_f}{D_f\lambda_{\max}^{2-D_f}}\frac{\rho A_s j^2\phi_a}{1-\xi^{2-D_f}}\left[j^{-D_f}-\left(j+\Delta\lambda\right)^{-D_f}\right] \\ &+\sum_{j=\lambda_t+\Delta\lambda}^{\lambda_{\max}}\frac{2-D_f}{D_f\lambda_{\max}^{2-D_f}}\frac{\rho A_s H j^2\phi_c}{1-\xi^{2-D_f}}\left[j^{-D_f}-\left(j+\Delta\lambda\right)^{-D_f}\right] \end{aligned} \tag{25}$$

The second model of spontaneous imbibition with gravity (Cai et al., 2012) is described as:

$$M(t) = \frac{\chi}{\psi}\left\{1+W\left[-e^{-1-\left(\psi^2/\chi\right)t}\right]\right\}$$

$$\begin{aligned} \chi &= \frac{\sigma\cos\theta}{8\mu\tau_{av}^2}\frac{2-D_f}{3-D_f}\frac{\left(\rho A_s\phi_a\right)^2\lambda_{\max}}{1-\phi_a}, \\ \psi &= \frac{\rho^2 A_s g}{32\mu\tau_{av}^2}\frac{2-D_f}{4-D_f}\frac{\phi_a\lambda_{\max}^2}{1-\phi_a} \end{aligned} \tag{26}$$

4. Results and discussion

Table 1 proposes the predictions of fluid imbibition mass with different imbibition times and interval numbers on the conditions of $A_s=3$ cm^2, $\theta=30°$, $H=40$ cm, $\rho=1$ g/cm^3,

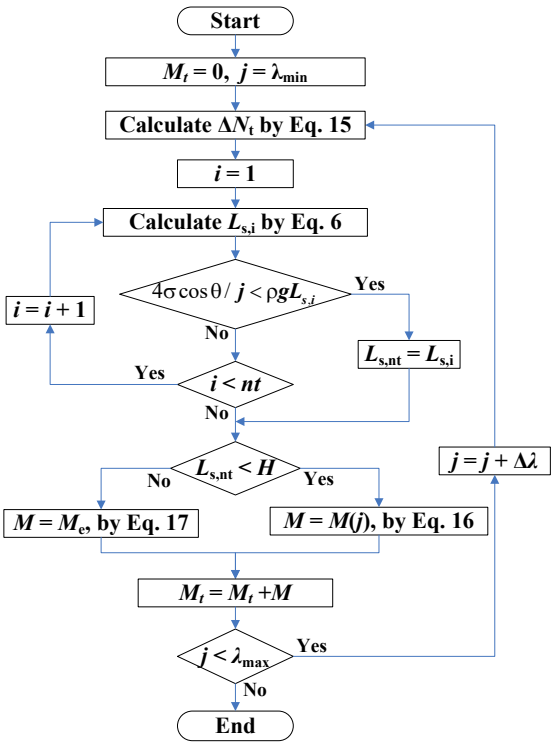

Fig. 3. Logic procedure for semi-analytical equation while considering gravity.

Table 1. Predictions of imbibition mass for different imbibition times and interval numbers.

t (s)	nt				
	100	250	500	1000	2000
1000	19.2877 g	19.2792 g	19.2764 g	19.2750 g	19.2744 g
5000	35.4247 g	35.4219 g	35.4210 g	35.4206 g	35.4204 g
10000	40.4941 g	40.4930 g	40.4927 g	40.4925 g	40.4924 g

$\phi_c = 0.2$, $D_{av} = 0.02$ cm, $\sigma = 0.727$ mN/cm, $\mu = 1$ mPa·s and $\xi = 0.01$. From the table, we can infer that the converged imbibition mass is reached when the interval number is more than 1000 for different imbibition times. Since the prediction of imbibition mass at $nt = 1000$ is almost the same as that at $nt = 500$ or $nt = 2000$, the prediction variance between $nt = 1000$ and $nt = 2000$ is less than 0.1%. Consequently, this paper limits the interval number nt to not less than 1000 for different imbibition times.

The variation of fractal tortuosity dimension D_t with the effective porosity ϕ_c is shown in Fig. 4. As seen in the figure, the value of D_t gradually drops with the increase of ϕ_c, and stays in the range of 1.0 to 1.11 when the effective porosity ϕ_c is between 0.2-0.9. The Eq. (4) indicates that the rising straight length of fluid column versus time follows the relationship $L_s(t) \sim t^{1/2D_t}$, and the time exponent equals to $2D_t$; the process follows $L_s(t) \sim t^{1/2}$ only for a straight capillary ($D_t = 1$) (Lucas, 1918; Washburn, 1921). From Eq. (4) it is clear that the time exponent of the capillary imbibing process is the reciprocal of $2D_t$. The parameter D_t is generally a function of

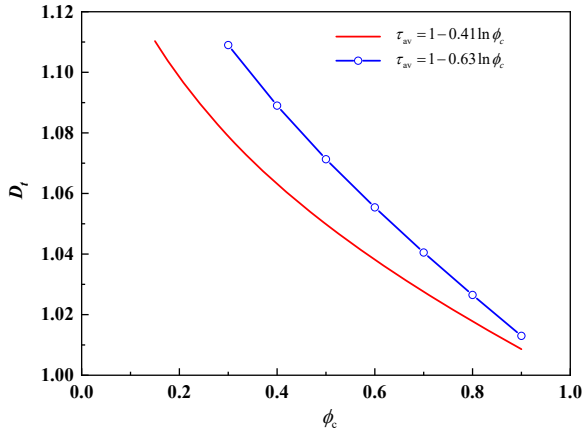

Fig. 4. Variation of fractal tortuosity dimension D_t with effective porosity ϕ_c, $\xi = 0.01$.

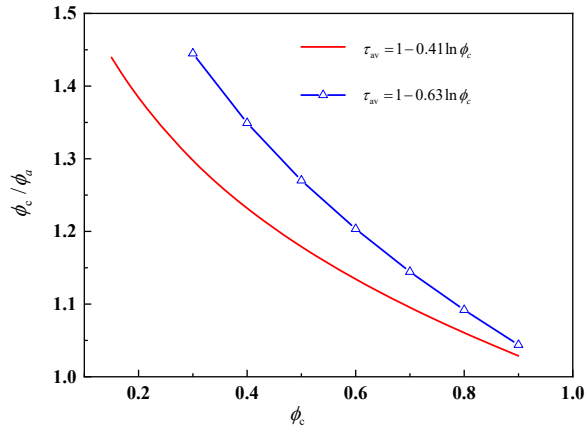

Fig. 5. Difference between areal porosity ϕ_a and effective porosity ϕ_c, $\xi = 0.01$.

porosity and rises with the reduction of porosity Xu and Yu, 2008), thus the time exponent increases with rising porosity. Since $1 < D_t < 1.11$, the time exponent is in the range of 0.45-0.5. Therefore, Eq. (4) in the present paper is more precise than the LW law (Lucas, 1918; Washburn, 1921).

Fig. 5 presents the difference between the areal porosity ϕ_a and the effective porosity ϕ_c. It can be seen that the ratio of ϕ_c to ϕ_a decreases with the increase of ϕ_c, and that ϕ_c is always larger than ϕ_a. This result disagrees with previous researches that ignored the difference between the effective porosity ϕ_c and the areal porosity ϕ_a (Yu and Cheng, 2002; Cai et al., 2012). Fig. 5 indicates that ϕ_a is about 77% of ϕ_c when $\phi_c = 0.3$, which demonstrates that the difference between ϕ_a and ϕ_c is not negligible.

Fig. 6 demonstrates the comparison between the areal porosity ϕ_a and the average areal porosity ϕ'. The value of ϕ_a or ϕ' rises with the increase of ϕ_c, and ϕ_a is larger than ϕ' when the value of ϕ_c is kept unchanged. This is not coherent with the correlation for areal porosity $\phi' = \phi_c / \tau_{av}$ obtained by Shi et al. (2018). Fig. 6 indicates that ϕ' is about 87% of ϕ_a when $\phi_c = 0.3$. And this suggests that the difference between ϕ_a and ϕ' cannot be ignored.

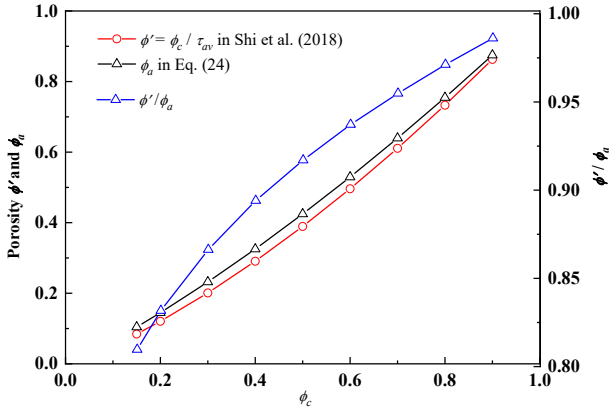

Fig. 6. Difference between areal porosity ϕ_a and average areal porosity ϕ'.

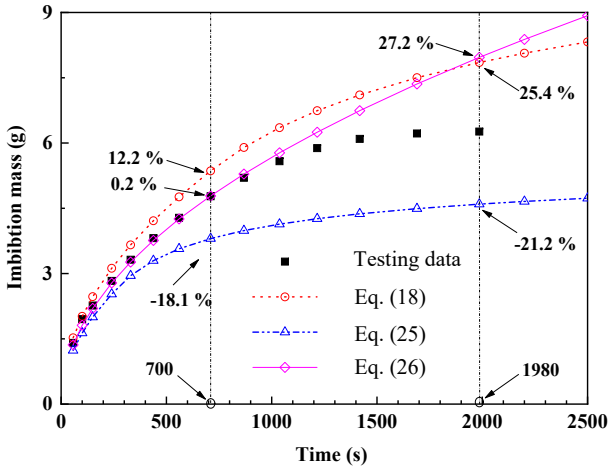

Fig. 7. Comparison of water imbibition mass while considering gravity versus time among three equations for the experimental data of Berea sandstone; $\phi_c = 0.15$, $D_{av} = 0.0034$ cm, $A_s = 3.14$ cm^2, $\theta = 26°$, $H = 11$ cm, $\sigma = 0.727$ mN/cm, $\rho = 1$ g/cm^3, $\mu = 1$ mPa·s, $\xi = 0.01$.

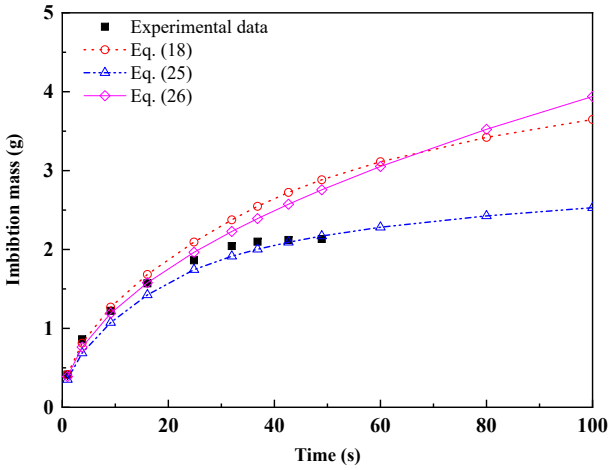

Fig. 8. Comparison of water imbibition mass while considering gravity versus time among three equations for the experimental data of Bentheim core; $\phi_c = 0.23$, $D_{av} = 0.0015$ cm, $A_s = 5.15$ cm^2, $\theta = 0°$, $H = 2.56$ cm, $\sigma = 0.727$ mN/cm, $\rho = 1$ g/cm^3, $\mu = 1$ mPa·s, $\xi = 0.01$.

Figs. 7 and 8 present the comparison of the imbibed mass of water with gravity versus time by different equations by using the experimental data of Berea sandstone (Schembre et al., 1998) and Bentheim cores (Olafuyi et al., 2007), respectively. It is observed that all of these three models fit the testing data well in the initial period of the imbibing process, but after a while, the testing data of imbibed mass are lower than the predictions of the model Eq. (18). These discrepancies can be explained as follows: during the derivation of the theoretical model, we assume that all capillaries can successfully extend from the bottom surface to the top surface of the rock sample, as shown in Fig. 2. However, for the real testing samples with regular shapes, such as cylindrical samples in Berea sandstone (Schembre et al., 1998) and Bentheim cores (Olafuyi et al., 2007), not all capillaries can extend their tortuous tubes from the bottom surface to the top surface of the testing samples, and a few capillaries inevitably fail to reach the top surface, therefore the imbibition water in these capillaries flows out from the side surface of the test samples. This will lead to a lower true imbibition water mass in testing as compared with the theoretical predictions.

From Figs. 7 and 8, we can also establish that, for a short imbibition time $t = 700$ s, the prediction variance of Eq. (26) is about 0.2%, the variance of Eq. (25) is about negative 18.1%, and that of Eq. (18) is about 12.2%. In other words, the model prediction of Eq. (26) is the best for short imbibition time among the three models compared with the testing data (Schembre et al., 1998). For a long imbibition time $t = 1980$ s, the prediction variance of Eq. (26) is about 27.2%, the variance of Eq. (25) is about negative 21.2%, and that of Eq. (18) is about 25.4%. Namely, among these three models, the prediction trend of Eq. (26) and Eq. (18) for a longer imbibition time is highly similar compared with that of Eq. (25).

Figs. 9(a) and 9(b) present the comparison of critical diameters between Eq. (12) of the present model and the model of Shi et al. (2018). It is observed that, with the increase of imbibition time, the prediction of critical diameter by Eq. (12) of the present model is higher than that of Shi et al. (2018). It is worth noting that, when the effective porosity ϕ_c and characteristic diameter D_{av} are given, the maximum diameter of capillary can be obtained by Eq. (19). Fig. 9(b) shows that, when $\lambda_{max} = 0.00599$ cm in Eq. (12), the imbibition time hits the critical time (about 1560 s), and the imbibition of the capillary with λ_{max} begins to face the critical diameter. In other words, the capillary pressure equals to the gravity pressure at this moment, and the imbibition process begins to cease. When the imbibition time exceeds 1560 s, the imbibition process terminates in the capillaries with diameters in the range of $\lambda_{max} > \lambda > \lambda_c$. For the model of Shi et al. (2018), however, the critical time is only about 740 s, which means that the beginning terminal time of the imbibition process in that model is earlier than that in Eq. (12) of this paper. As illustrated in Figs. 7 and 8, this can explain why the fluid imbibition mass predictions of Eq. (18) of this paper are higher than those of Shi et al. (2018).

Eq. (15) indicates that the total number of capillaries with

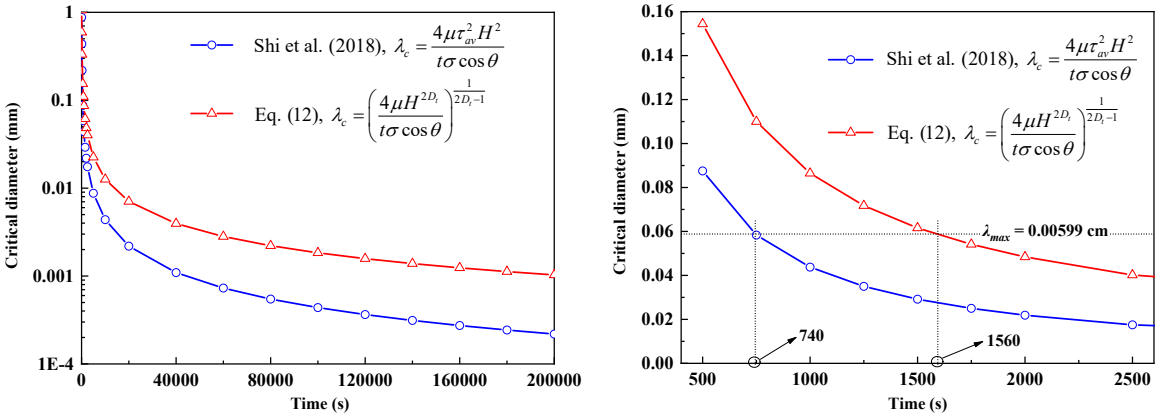

Fig. 9. Comparison of critical diameters between two equations while considering gravity; $\phi_c = 0.2$, $D_{av} = 0.02$ cm, $A_s = 5.15$ cm^2, $\theta = 30°$, $H = 50$ cm, $\sigma = 0.727$ mN/cm, $\rho = 1$ g/cm^3, $\mu = 1$ mPa·s, $\xi = 0.01$.

same diameter is proportional to the value of areal porosity ϕ_a or ϕ'. Based on the parameters given in Table 2, Table 3 compares the total number ΔN_t of capillaries in Eq. (15) with that of Shi et al. (2018). Table 3 demonstrates that the total number ΔN_t in Eq. (15) is greater than that of Shi et al. (2018). The reason for this might be that the areal porosity is $\phi_a = 0.145$, the average areal porosity is $\phi' = 0.120$, and ϕ' is about 83% of the value of ϕ_a, which exactly agrees with the ratio of about 87% of the total number in Eq. (15) to that in Shi et al. (2018).

The total imbibition mass $M(\lambda)$ of fluid in the capillaries with diameter in the range of λ to $\lambda + \Delta\lambda$ can be calculated by Eq. (16). Fig. 10 displays the effect of the ratio of $\lambda/\lambda_{\max}$ on the value of $M(\lambda)$. From Fig. 10, we can find that the value of $M(\lambda)$ decreases with the increase of $\lambda/\lambda_{\max}$. This can be explained by the fact that the total number of small diameter capillaries is far greater than that of large diameter capillaries, thus even the cross section of a single capillary with a small diameter is lower than that of capillary with a big diameter, the imbibition mass $M(\lambda)$ still decreases with the increase of capillary diameter.

It can also be inferred from Fig. 10 that the value of $M(\lambda)$ of our model is slightly higher than that of Shi et al. (2018) for a shorter imbibition time of 1000 s, whereas the value of $M(\lambda)$ of our model is much higher than that of Shi et al. (2018) for a longer imbibition time of 10000 s. This is because the total number ΔN_t in Eq. (15) is greater than that in Shi et al. (2018) due to the difference between the areal porosity ϕ_a and ϕ', which leads to the underestimation of fluid imbibition mass in the capillaries by the model of Shi et al. (2018). The difference is not obvious for the initial imbibing period, however, with the increase of imbibition time, the difference gradually expands and the value of $M(\lambda)$ of our model will be much higher than that of Shi et al. (2018) for a longer imbibition time.

Fig. 11 compares the imbibition mass among three different equations on the condition of gravity pressure. The figure demonstrates that, with the increase of rock sample height H, the imbibition mass of Eq. (18) and of Eq. (25) always increases, whereas the imbibition mass of Eq. (26) is independent from H for a longer imbibition time. We also can find that, among these three equations, the imbibition mass of Eq. (18) is the largest, and the imbibition mass of Eq. (25) is the smallest. These discrepancies are due to the fact that the prediction model in Eq. (26) ignores the large difference between the effective porosity ϕ_c and the areal porosity ϕ_a. Moreover, although the prediction model in Eq. (25) considers this disparity, Eq. (25) ignores the obvious difference between areal prosity ϕ_a and ϕ'. All these factors lead to the discrepan-

Table 2. Parameter values.

Parameters	Valule	Parameters	Valule
ϕ_c	0.2	θ	30°
ϕ_a	0.145	H	40 cm
ϕ'	0.12	σ	0.727 mN/cm
D_f	1.65	ρ	1 g/cm^3
D_{av}	0.02 cm	μ	1 mPa·s
$\lambda_{\max}$	0.00599 cm	ξ	0.01
A_s	3 cm^2	Δt	1 s

Table 3. Comparison of the total number ΔN_t of capillaries with the same diameter while considering gravity.

$\lambda/\lambda_{\max}$	0.05	0.1	0.2	0.3	0.4	0.5	0.6	0.7	0.8
ΔN_t in Shi et al. (2018)	7791	1167	175	57.6	26.2	14.2	8.6	5.7	3.9
ΔN_t in Eq. (15)	8993	1347	202	66.5	30.2	16.4	10.0	6.5	4.5
Ratio	0.87	0.87	0.87	0.87	0.87	0.87	0.86	0.88	0.87

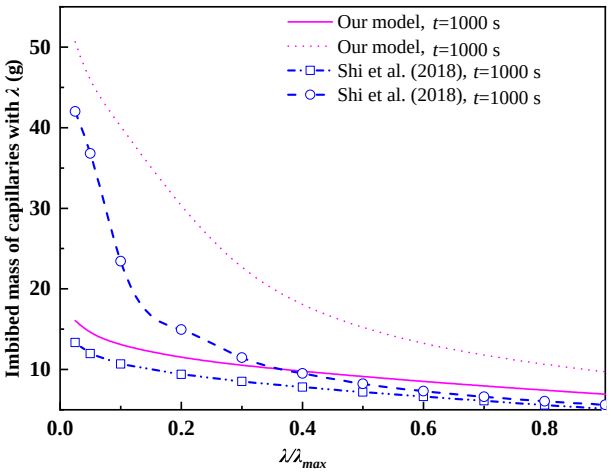

Fig. 10. Comparison of imbibition mass of capillaries with the same diameter between two models while considering gravity; $\phi_c = 0.2$, $D_{av} = 0.02$ cm, $A_s = 3$ cm^2, $\theta = 30°$, $H = 40$ cm, $\sigma = 0.727$ mN/cm, $\rho = 1$ g/cm^3, $\mu = 1$ mPa·s, $\xi = 0.01$.

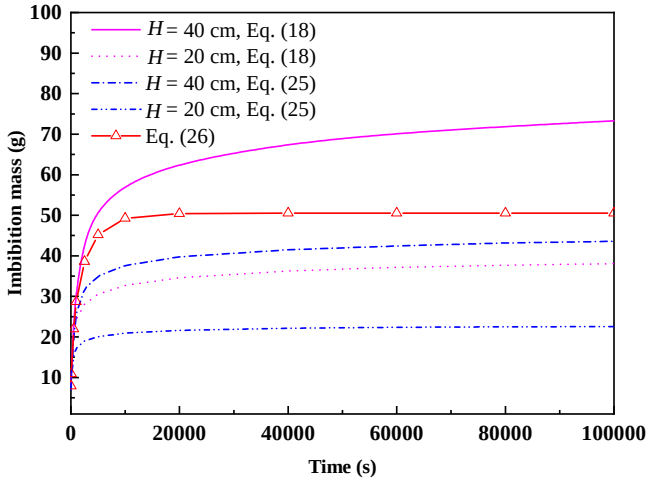

Fig. 11. Comparison of imbibition mass among three equations while considering gravity; $\phi_c = 0.3$, $D_{av} = 0.02$ cm, $A_s = 3$ cm^2, $\theta = 30°$, $\sigma = 0.727$ mN/cm, $\rho = 1$ g/cm^3, $\mu = 1$ mPa·s, $\xi = 0.01$.

cies of imbibition mass prediction among the three equations.

Fig. 12 presents the results of Eqs. (18) and (11) with the parameter H. The difference among the displayed curves is due to the gravity pressure. It can be seen that the difference is slight with a small H value of 0.4 m, while the difference seems more significant with a larger H value of 2 m. This means that the gravitational pressure can not only equilibrate the capillary pressure, but also cease the fluid imbibing process before it reaches the top surface of the rock sample. In other words, for rock samples with greater height, the effect of gravitational pressure is important, and Eq. (11) will lead to a more considerable overestimation of the imbibition mass.

5. Conclusions

The significant difference between this work and the previous researches is that we consider the obvious distinction between the effective porosity and the areal porosity. An implicit equation for fractal tortuosity and a modified correlation for the areal porosity are proposed, and the analysis results show that the value of areal porosity is always greater than that of the average areal porosity, and the difference between the areal porosity and the effective porosity is too large to be ignored. A semi-analytical prediction model of fluid imbibition mass with gravity pressure is derived, and its validity is proved by comparing the testing data with previous studies. The imbibition mass predictions of three different models have also been discussed.

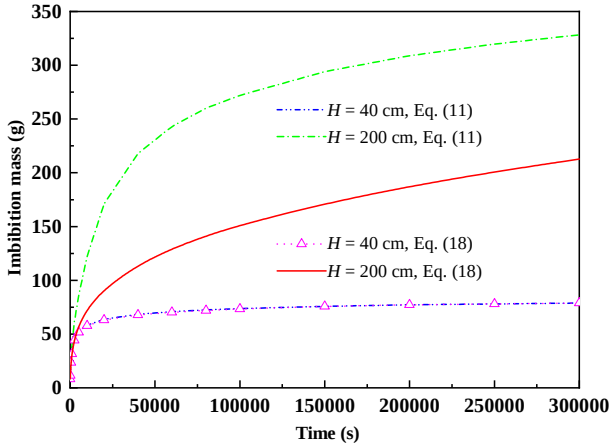

Fig. 12. Comparison of water imbibition mass between considering and ignoring gravity; $\phi_c = 0.3$, $D_{av} = 0.02$ cm, $A_s = 3$ cm^2, $\theta = 30°$, $\sigma = 0.727$ mN/cm, $\rho = 1$ g/cm^3, $\mu = 1$ mPa·s, $\xi = 0.01$.

Nomenclature

A_s = total cross-section area of rock sample, m^2
A_u = cross-section area of cubic unit cell, m^2
D_{av} = characteristic particle diameter, m
D_f = pore fractal dimension, dimensionless
D_t = tortuosity fractal dimension, dimensionless
L_s = straight distance of fluid column, m
L_t = actual tortuous distance of fluid column, m
L_u = side length of cubic unit cell, m
m = imbibed mass in a single capillary, kg
M = imbibed mass in a capillary bundle, kg
M_e = equilibrated mass in a capillary bundle, kg
M_t = total imbibed mass of rock sample, kg
N = total number of pores, dimensionless
ΔN_t = number of capillaries with diameter value in the range of λ to $\lambda + \Delta\lambda$, dimensionless
nt = total interval number of imbibition time, s
t = imbibition time, s
V_p = particle volume of cubic unit cell, m^3
V_u = total volume of cubic unit cell, m^3
θ = contact angle, °
τ_{av} = average tortuosity of capillary, dimensionless
σ = surface tension, N/m
ρ = density of wetting phase, kg/m^3
λ_{av} = average capillary diameter, m
λ_c = critical diameter of capillary, m
λ_{max} = maximum capillary diameter, m
λ_{min} = minimum capillary diameter, m

λ_t = threshold diameter of capillary, m
ϕ_a = areal porosity of porous media, dimensionless
ϕ_c = effective porosity of porous media, dimensionless
ϕ' = average areal porosity, ratio of ϕ_c to τ_{av}, dimensionless
μ = absolute viscosity of wetting phase, Pa·s
ξ = ratio of λ_{min} to λ_{max}, dimensionless

Acknowledgement

The authors sincerely appreciate the support of the Natural Science Foundation of Jiangsu Province (Grant No. BK20140924).

Conflict of interest

The authors declare no competing interest.

References

Ashraf, S., Phirani, J. Capillary displacement of viscous liquids in a multi-layered porous medium. Soft Matter, 2019, 15(9): 2057-2070.

Balankin, A. S., Elizarraraz, B. E. Hydrodynamics of fractal continuum flow. Physical Review E, 2012, 85(2): 025302.

Cai, J., Hu, X., Standnes, D. C., et al. An analytical model for spontaneous imbibition in fractal porous media including gravity. Colloids and Surfaces A: Physicochemical and Engineering Aspects, 2012, 414: 228-233.

Cai, J., Perfect, E., Cheng, C., et al. Generalized modeling of spontaneous imbibition based on Hagen-Poiseuille flow in tortuous capillaries with variably shaped apertures. Langmuir, 2014, 30(18): 5142-5151.

Cai, J., Yu, B. A discussion of the effect of tortuosity on the capillary imbibition in porous media. Transport in Porous Media, 2011, 89(2): 251-263.

Cai, J., Yu, B., Mei, M., et al. Capillary rise in a single tortuous capillary. Chinese Physics Letters, 2010a, 27(5): 054701.

Cai, J., Yu, B., Zou, M., et al. Fractal characterization of spontaneous co-current imbibition in porous media. Energy & Fuels, 2010b, 24(3): 1860-1867.

Cai, J., Yu, B., Zou, M., et al. Fractal analysis of invasion depth of extraneous fluids in porous media. Chemical Engineering Science, 2010c, 65(18): 5178-5186.

Dudek, M., Bertheussen, A., Dumaire, T., et al. Microfluidic tools for studying coalescence of crude oil droplets in produced water. Chemical Engineering Science, 2018, 191: 448-458.

Elizalde, E., Urteaga, R., Berli, C. Rational design of capillary-driven flows for paper-based microfluidics. Lab on a Chip, 2015, 15(10): 2173-2180.

Gao, L., Yang, Z., Shi, Y. Experimental study on spontaneous imbibition characteristics of tight rocks. Advances in Geo-Energy Research, 2018, 2(3): 292-304.

Li, K., Zhao, H. Fractal prediction model of spontaneous imbibition rate. Transport Porous Media, 2012, 91(2): 363–376.

Liu, G., Zhang, M., Ridgway, C., et al. Spontaneous inertial imbibition in porous media using a fractal representation of pore wall rugosity. Transport in Porous Media, 2014, 104(1): 231-251.

Liu, S., Ni, J., Wen, X., et al. A dual-porous and dual-permeable media model for imbibition in tight sandstone reservoirs. Journal of Petroleum Science and Engineering, 2020, 194: 107477.

Lucas, R. Rate of capillary ascension of liquids. Kolloid-Zeitschrift, 1918, 23: 15-22.

Nishikawara, M., Otani, K., Ueda, Y., et al. Liquid–vapor phase behavior and operating characteristics of the capillary evaporator of a loop heat pipe at start-up. International Journal of Thermal Sciences, 2018, 129: 426-433.

Olafuyi, O. A., Cinar, Y., Knackstedt, M. A., et al. Spontaneous imbibition in small cores. Paper SPE 109724 Presented at the Asia Pacific Oil and Gas Conference and Exhibition, Jakarta, Indonesia, 30 October-1 November, 2007.

Orlando, C. E., Ruben, E. S., Krishna, D. P. N., et al. Directional displacement of non-aqueous fluids through spontaneous aqueous imbibition in porous structures. Chemical Engineering Science, 2020, 228: 115959.

Pia, G., Sanna, U. A geometrical fractal model for the porosity and thermal conductivity of insulating concrete. Construction and Building Materials, 2013, 44: 551-556.

Schembre, J. M., Akin, S., Castanier, L. M., et al. Spontaneous water imbibition into diatomite. Paper SPE 46211 Presented at the SPE Western Regional Meeting, Bakersfield, California, 10-13 May, 1998.

Shi, Y., Yassin, M. R., Dehghanpour, H. A modified model for spontaneous imbibition of wetting phase into fractal porous media. Colloids and Surfaces A: Physicochemical and Engineering Aspects, 2018, 543: 64-75.

Washburn, E. W. The dynamics of capillary flow. Physical Review, 1921, 17(3): 273-283.

Wijshoff, H. Drop dynamics in the inkjet printing process. Current Opinion in Colloid & Interface Science, 2018, 36: 20-27.

Wu, J., Yu, B. A fractal resistance model for flow through porous media. International Journal of Heat and Mass Transfer, 2007, 50(19-20): 3925-3932.

Xie, J., Gao, M., Zhang, R., et al. Experimental investigation on the anisotropic fractal characteristics of the rock fracture surface and its application on the fluid flow description. Journal of Petroleum Science and Engineering, 2020, 191: 107190.

Xu, P., Yu, B. Developing a new form of permeability and Kozeny-Carman constant for homogeneous porous media by means of fractal geometry. Advances in Water Resources, 2008, 31(1): 74-81.

Yu, B., Cai, J., Zou, M. On the physical properties of apparent two-phase fractal porous media. Vadose Zone Journal, 2009, 8(1): 177-186.

Yu, B., Cheng, P. A fractal permeability model for bi-dispersed porous media. International Journal of Heat and Mass Transfer, 2002, 45(14): 2983-2993.